LAWRENCE
LIVERMORE
NATIONAL
LABORATORY

UCRL-JRNL-221255

Mesoscale modeling of irreversible volume growth in powders of anisotropic crystals

R. Gee, A. Maiti, L. Fried

May 9, 2006

Applied Physics Letters

Updated October 14, 2003

Mesoscale modeling of irreversible volume growth in powders of anisotropic crystals

Richard Gee, Amitesh Maiti*, and Laurence Fried

Lawrence Livermore National Laboratory, University of California, Livermore, CA 94551

Abstract

Careful thermometric analysis (TMA) on powders of micron-sized triamino-trinitrobenzene (TATB) crystallites are shown to display irreversible growth in volume when subjected to repeated cycles of heating and cooling. Such behavior is counter-intuitive to typical materials response to simulated annealing cycles in atomic-scale molecular dynamics. However, through coarse-grained simulations using a mesoscale Hamiltonian we quantitatively reproduce irreversible growth behavior in such powdered material. We demonstrate that irreversible growth happens only in the presence of intrinsic crystalline anisotropy, and is mediated by particles much smaller than the average crystallite size.

Keywords: Mesoscale modeling, Irreversible growth, Granular systems

PACS: 65.40.De, 65.60.+a, 47.11.Mn, 47.11.St

* Corresponding author, E-mail: *maiti2@llnl.gov*

Standard simulation methods in materials science and engineering can be roughly classified into three groups: (1) atomic-level molecular dynamics or Monte Carlo, based on forces obtained from quantum mechanics or classical potentials; (2) continuum-scale finite-elements modeling, which could be grid or particle based; (3) an emerging field of mesoscale modeling, aimed at analyzing phenomena at intermediate length and time-scales. Although many challenges still remain, the first two simulation methods are quite mature. In comparison, serious inroads into mesoscale methods have started relatively recently, being prompted by new problems in composite science, geophysics, biomaterials, and diverse applications of nanotechnology.

Even within the field of mesoscale modeling there are application areas where the methodology is more developed than others. This is particularly true for "soft" materials like simple molecular liquids to complex polymeric fluids, blends, and melts where statistical mechanical theories have led to fairly robust algorithms based on classical density functionals [1] and bead-spring models [2]. However, examples abound where such methodologies are not readily applicable, e.g., biomaterials like bone and teeth composed of ceramic crystallites within a soft protein-like matrix [3], or shells (e.g., nacre) comprising brick-and-mortar like arrangement of aragonite crystals with very little soft matrix [3], or geological systems like the earth's crust consisting of plates floating on a relatively softer mantle [4], or composites where clay nanoparticles are embedded within a predominantly soft polymeric environment [5], or plastic-bonded explosives where crystallites of high-energy molecules are bonded with a small amount of polymeric binder [6]. The presence of a "hard" component in the preceding examples creates several modeling challenges: (1) hardness in potential may result in a reduction of the effective time-step, which can severely limit timescale of phenomena to be studied; (2) in the absence of general guiding principles, e.g., an equivalent of the Flory-Huggins theory [7] for hard systems accurate mesoscale parameters would typically require well-characterized experimental data on individual components as well as their interactions, which may not be readily available.

In this Letter we consider the specific example of a plastic-bonded explosive (PBX) consisting of a pressed powder of the energetic material 1, 3, 5-triamino-2, 4, 6-trinitrobenzene (TATB) bonded by a small amount (~ 5% by weight) of polymer [8]. The single-crystal of TATB in its predominant polymorphic form has a layered structure (like graphite), and pressed powder TATB explosives, with or without polymer binder has previously been found to undergo the interesting phenomenon of

irreversible growth upon repeated cycles of cooling and heating [8]. Irreversible growth is also found to occur in other anisotropic materials like boron-nitride and graphite [9]. The phenomenon of irreversible growth is remarkably contradictory to common intuition by which one expects to see a lowering of system energy through gradual compaction of the powder [10]. Our challenge was to develop a mesoscale model that describes the essential interactions at the micron scale, and is able to reproduce the irreversible growth phenomenon with quantitative accuracy.

In order to obtain a consistent set of quantitatively accurate data, we performed careful thermometric analysis on well-prepared samples in which TATB particles were bonded with a few % of the copolymer Kel-F-800 (cholorotrifluoroethylene/vinylidine 3:1). The linear expansion data was obtained by a thermo-mechanical analyzer (TA instruments, model 2940) using a cylindrical sample of 6.35 mm diameter and 6.62 mm length, precision machined from a billet pressed material with considerable care taken to ensure that the ends were flat and parallel. The temperature was cycled within a range of approximately -54 to +74 ºC, at a ramp rate of 3 ºC per minute, with ten minute dwell times at each extreme. Fig. 1(a) displays, for sample #6, the fractional length-variations as a function of temperature over the first 11 thermal cycles. Fig. 1(b) displays, for five different samples, the room-temperature data extracted from each thermal cycle. All of the samples clearly display irreversible growth, with amounts varying between 0.3-0.8%. During the pressing, different parts of the billet are subject to different stress fields. Therefore, the sample-to-sample variation in irreversible growth is likely due to differences in the density composition (i.e. particle size-distribution) of the powder, as well as due to possible differences in orientational alignment of the particles relative to their basal planes.

Fig. 2(a) illustrates the experimentally determined, triclinic structure of TATB unit cell. It is a layered structure with triclinic space group P-1 [11], and exhibits significant anisotropy when comparing properties within and perpendicular to the basal planes, which are parallel to the XY plane of Fig. 2(a) [12]. In particular, the coefficient of thermal expansion (CTE) exhibits significantly larger value perpendicular to the basal plane as compared to in-plane [12, 13]. In order to describe particles of linear dimension ranging from 1 to several microns, it was natural to coarse-grain a cubic “block” of crystal material into a single meso “bead”, with the cube edges parallel to the X, Y and Z axes of Fig. 2(a). To incorporate the intrinsic crystalline anisotropy of the original material in the cubic “meso”

crystal, we designated meso beads in alternate layers parallel to the XY plane as "A" and "B" beads (Fig. 2(b)), and differentiated between like (i.e. A-A and B-B) and unlike (i.e. A-B) bonds. To obtain realistic shapes of meso crystallites, we computed the average equilibrium morphology [14, 15] of the original molecular crystal using an accurate inter-atomic potential developed for this system [16] (Fig. 2(c)). Then we created a meso representation of such crystallites (Fig. 2(d)) by cleaving appropriate planes from the meso crystal model of Fig. 2(b). It should be noted that the Morphology theory only yields the average shape of crystallites [14], and not the size. Therefore, in general it is necessary to build an ensemble of meso particles of various sizes to create an experimental representation of a powdered sample. Fig. 3 displays a representative example of several ensembles used in our simulations. Fig. 3(a) illustrates an ensemble consisting only of larger crystallite particles, which is an inefficiently packed system with a significant amount of void space. Fig. 3(b), in which inter-crystallite voids of Fig. 3(a) are packed with small TATB particles (represented by small cubes), is a much more realistic representation of an experimental pressed powder system, where high pressure is employed to achieve a density as high as 96% of the theoretical maximum. It is important to note that such a high experimental packing density could only be achieved through the presence of small particles, either present originally in the sample, or created by breaking of larger crystallites under pressure [17]. Hereafter we refer to structures in Fig. 3(b) as a *pressed-powder*. To create such structures we use a random packing program in which we first decide on a size distribution of crystallites, and pack starting from the biggest particles, and progressively go down in size, and finally fill inter-crystallite space with the smallest cubes in order to achieve the experimental packing fraction. In the plastic-bonded material (PBX) the polymeric binder is known to form thin coats around the TATB particles, and is therefore best represented through modification of inter-crystallite interaction energies, as discussed below.

Although no formal theory of irreversible growth in anisotropic material exists in the literature, there have been a few suggested mechanisms, including the excitation of libration modes, and build-up of high internal pressures, both of which can potentially lead to intra-crystalline voids [8, 12]. However, in the temperature range of our interest (-54 to 74 °C) the libration mechanism is unlikely, as is supported by atomistic simulations using a recently-developed forcefield [16], as well as X-ray observations [11]. We, therefore, explore a mechanism in which each crystallite can vibrate, translate, and rotate, but otherwise has its shape and size intact upon thermal cycling. Such a mechanism is

natural given that the intra-crystallite bonding interactions are much stronger than the inter-crystallite nonbond interaction between two external surfaces. For bead-bead interaction *within* a meso-crystallite we chose explicit nearest-neighbor bond and angle-energy terms in the simple *harmonic* form:

$$E(b_{\alpha\beta}) = K_{bond}(b_{\alpha\beta} - b^0{}_{\alpha\beta})^2, \text{ and } E(\theta_{\alpha\beta\gamma}) = K_{angle}(\theta_{\alpha\beta\gamma} - \theta^0{}_{\alpha\beta\gamma})^2, \quad (1)$$

where each of the subscripts α, β, γ could be bead types *A* or *B*, while the weaker *inter-crystallite* bead-bead interaction was chosen to be of the Morse functional form:

$$E(r_{ij}) = D[\{1 - e^{-\alpha(r_{ij} - r_0)}\}^2 - 1] \quad (2)$$

The Morse function is sharper and more localized than the more commonly used Lennard-Jones 6-12, and is therefore more appropriate for describing the hard interaction between the surfaces of solid crystallites representing the powdered material – the parameters *D* and α can be interpreted as the *depth* and *inverse range* of the interaction respectively. For the PBX material one needs to model an additional component, i.e., the polymer binder, which essentially fills the inter-crystallite space as a thin coat. A simple way to represent such a material is through a larger value of *D* and a smaller value of α as compared to the pure pressed-powder system without binder [18].

In the absence of anharmonicity in the bond terms in Eq. (1), one needs to incorporate thermal expansion by making the equilibrium bond separation T-dependent, i.e.,

$$b^0{}_{\alpha\beta}(T) = b^0{}_{\alpha\beta}(T_L) + C^{Th}{}_{\alpha\beta}(T - T_L), \quad (3)$$

where T_L is the lower limit of the temperature range of our interest, and $C^{Th}{}_{\alpha\beta}$ is the experimentally measured CTE. Because of previously-stated anisotropy of TATB, the in-plane CTE ($C^{Th}{}_{AA} = C^{Th}{}_{BB}$) is much smaller than the CTE perpendicular to the basal planes ($C^{Th}{}_{AB}$) [19].

Table 1 lists the values of various parameters defined in Eqs. (1-3) and how they scale with bead-size *N* [20]. Large crystallites in our experimental samples are of dimensions 20-50 μm, which sets the basic length-scale, governed by b^0, to 1 μm. The parameter K_{bond} is chosen to ensure that the amplitude of oscillation ~ $\sqrt{k_B T / K_{bond}}$ is a small fraction (i.e. < 8%) of the inter-bead distance. The same logic holds for K_{angle}. Our choice makes the fastest oscillation time $\tau_{fastest} \sim 2\pi / \sqrt{K_{bond}} = 0.6$ in reduced

units. At the atomistic scale, $\tau_{fastest}$ ~ 10^{-13}-10^{-12} *s*. Thus, at our mesoscale, $\tau_{fastest}$ ~ 10^{-3} – 10^{-2} *s* (using the $N^{5/6}$ scaling [20]). The MD time-step used is two orders of magnitude smaller than $\tau_{fastest}$. As for the Morse parameters, the inter-crystalline r_0 is chosen as slightly (i.e., 30%) larger than the intra-crystalline b^0, while the Morse parameters α and *D* are chosen such that they satisfy the constraints: (1) $D << K_{bond}(b^0)^2$, (2) $\delta \sim \sqrt{k_B T / D\alpha^2} << r_0$, and (3) $D >> k_B T$, corresponding to the requirements that: (1) inter-crystallite interactions are much weaker than intra-crystallite interactions, (2) external surfaces do not approach to within a distance $(r_0 - \delta)$, where δ is a very small fraction of r_0, and (3) the cohesive energy maintains a proper physical density under ambient conditions. To satisfy conditions (1) and (3), we borrowed from the familiar concepts of molecular interactions, and chose *D* of the order of a hydrogen bond ~ 7-10 kcal/mol. To satisfy condition (2), we explored a few values in the range α = 10-60 μm^{-1}, corresponding to δ / r_0 ~ 3% or less. Larger values of α did not seem to affect the amount of irreversible growth (see Fig. 4 below).

With the bead-bead potential defined above, we carry out simulations to study volumetric growth induced upon repeated thermal cycling. To this end, we employed the classical molecular dynamics as implemented in the LAMMPS code [21]. The remarkably smooth curves of Fig. 1 are a result of averaging over a large number of crystallites that an experimental sample consists of, and so we had to consider fairly large computational cells as well. The total number of meso "beads" in our simulation cell was in the range 50000-100000, with the lower end corresponding to structures like Fig. 3(a) (with significant void space) and the upper end corresponding to pressed-powder systems, which were packed to 96% efficiency. The mesoscale simulations were carried out in two stages:

1. Equilibration: In this stage, the initially constructed sample was annealed at high temperatures by performing NPT dynamics for 10^8 steps, in order to eliminate voids as efficiently as we could achieve within the simulation time. This is equivalent to an equilibration run in standard molecular dynamics. The equilibrium bond-lengths were fixed at the low temperature value, and therefore the annealing run does not represent thermal cycling.

2. Thermal cycling: In this stage, the annealed sample was thermally cycled for several cycles. Each cycle consisted of raising the temperature from the low (-54 ^{0}C) to the high (74 ^{0}C) temperature in 7

steps, and then lowering the temperature reversibly in another 7 steps. At each temperature step the bond-lengths were expanded according to Eq. (2), and NPT dynamics was performed for 10^6 steps.

We performed the above thermal cycling procedure for several different ensembles over a range of interaction parameters D and α. From all these simulations we found that even under strong crystalline anisotropy systems as in Fig. 3(a) the growth curve is flat, i.e., *there is no irreversible growth in the absence of small particles*. Thus in Fig. 4, for concreteness, we focus on the results of one particular pressed-powder system consisting of a total of 73602 beads, out of which a fraction of ~ 30 % was small cubic particles.

Fig. 4(a) displays the growth curve when we artificially neglect the inherent anisotropy of TATB and use the same CTE in all directions [19]. Such a calculation, representative of all regular isotropic materials, conclusively demonstrates that *irreversible growth should be observed only in highly anisotropic materials*, especially the ones with layered structures. Fig. 4(b) displays the temperature variation of the cell-length (averaged over three dimensions) as a function of thermal cycling for parameter values D = 7 and α = 40, while Figs. 4(c, d) summarize the cycle-variation of room-temperature change in linear dimensions for different values of D and α. We note that: (i) the overall behavior of dimensional change as a function of thermal cycling (Fig. 4(b)) agrees well with experiment (Fig. 1(a)); (ii) for a wide range of parameter values the computed irreversible growth is within the experimentally observed range of Fig. 1(b); (iii) irreversible growth decreases with increasing D; (iv) irreversible growth increases with α, saturating at $\alpha \sim 40$ (30) for D = 7 (10) respectively. *If one simplistically interprets the presence of polymer as increasing D and/or decreasing α, it would imply smaller irreversible growth.* However, a more accurate analysis needs to consider additional physical properties of properties, e.g., glass-transition temperature, flow properties, and so on.

From analysis of structures before and after thermal cycling, it appears that irreversible growth happens by the movement of crystallites induced by anisotropic stress build up due to intrinsic crystalline anisotropy. In the isotropic case, all crystallites expand by the same fractional amount in all directions, and there is little residual stress that can drive volume growth. Anisotropy-generated local stress, in contrast, tends to drive crystallites from an initial pressed-powder configuration to one of a

large number of metastable states with slightly less compaction density. Such structures are of slightly higher energy than the original compacted configuration, but likely with higher configurational entropy. Due to the facetted particle shapes, such a movement is possible only in the presence of small particles, which effectively act as lubricants and allow the system to move out of the compacted geometry and explore the metastable phase space. In their absence, the crystallites get jammed [22], and there is no volume growth. Gravity-induced pressure-nonuniformity have previously been observed to lead to irreversible growth in a column of glass spheres subjected to thermal cycles [23], and such behavior analyzed with a simple model [24]. Entropic affects have also been attributed to irreversible growth in polycarbonate compacts [25].

In summary, we have developed a mesoscale model for a pressed-powder system, which: (1) borrows from atomic-scale interactions [26] and systematically scales up parameters for the length-scale of *microns* and time-scale of *seconds*; (2) quantitatively yields the phenomenon of irreversible growth under simulated thermal cycles; (3) conclusively demonstrates that irreversible growth does not happen in the absence of crystalline anisotropy; (4) provides the insight that such irreversible growth is mediated by particles much smaller than the average crystallite size; and (5) provides a simple parametric way to investigate the effect of polymer binder on powder morphology and growth. Preliminary simulations also indicate the same total irreversible volume growth even when the system is mechanically confined in one of the dimensions, in agreement with limited experimental data. Currently we are investigating the amount of irreversible growth as a function of the fraction of small particles in the ensemble. The approach developed here is general and robust, and should be useful in simulating the structural evolution of important materials systems in diverse science and engineering disciplines.

Acknowledgement: We would like to sincerely thank Drs. Bruce Cunningham and Arnie Duncan for giving access to unpublished data. The work was performed under the auspices of the U.S. Department of Energy by the University of California Lawrence Livermore National Laboratory under Contract W-7405-Eng-48.

References:

1. J.G.E.M. Fraaije, et al. *J. Chem. Phys.* **106**, 4260 (1997); G. H. Fredrickson, V. Ganesan, and F. Drolet, *Macromolecules* **35**, 16 (2002); S. C. Glotzer and W. Paul, *Annu. Rev. Matter. Res.* **32**, 401 (2002).

2. R. D. Groot and P. B. Warren, *J. Chem. Phys.* **107**, 4423 (1997); A. Maiti, J. Wescott, and G. Golbeck-Wood, *Int. J. Nanotechnology* **2**, 198 (2005); M. Karttunen, I. Vattulainen, A. Lukkarinen, eds. *Novel Methods in Soft Matter Simulations*, Springer (2004).

3. H. Gao, B. Ji, I. L. Jager, E. Arzt, and P. Fratzl, *Proc. Nat. Acad. Sci.* **100**, 5597 (2003), and references therein.

4. K. C. Kondie, *Earth as an evolving planetary system*, Elsevier Academic Press (2005).

5. T. J. Pinnavaia and G. W. Beall, eds., *Polymer-Clay Nanocomposites*, John Wiley & Sons (2000).

6. P. W. Cooper, *Explosives Engineering*, Wiley-VCH (1996).

7. M. Doi, *Introduction to Polymer Physics*, Oxford Science Publications (1996).

8. H. F. Rizzo, J. R. Humphrey, and J. R. Kolb, *Propellants Explos.* **6**, 57 (1981).

9. G. W. Hollenberg and R. Ruh, *AIP Conf. Proc.* **17**, 241 (1973).

10. F. X. Sanchez-Castillo and J. Anwar, *J. Chem. Phys.* **118**, 4636 (2003).

11. H. H. Cady and A. C. Larson, *Acta Crystallogr.*, Part 3, **18**, 485 (1965).

12. J. R. Kolb and H. F. Rizzo, *Propellants Explos.* **4**, 10 (1979).

13. Experimentally, the in-plane CTE are ~ 8 x 10^{-6} /K and 20 x 10^{-6} /K along the *a* and *b* axes, and ~ 250 x 10^{-6} /K normal to the basal plane [12].

14. The equilibrium morphology involves minimizing the total surface energy of the crystallite [15], and is obtained by Wulff construction from surface energies using Accelrys' code *Morphology*: See: http://www.accelrys.com/products/mstudio/modeling/crystallization/morphology.html

15. J. W. Gibbs, *Collected Works*, Longman, New York (1928).

16. R. H. Gee et al., *J. Chem. Phys.* **120**, 7059 (2004).

17. We have also developed non-bond models that allows for crystal fracture, and have obtained irreversible growth similar to those described in Fig. 4. Details are available as supplemental material, and will be published elsewhere.

18. We have also explored "softer" functional forms (e.g., Lennard-Jones) for polymer-polymer and polymer-TATB interactions. However, because of the amount of polymer in our system being low (< 5%) it did not lead to any significant difference in results. This point needs further consideration in systems with higher relative amount of the "soft" component.

19. In keeping with the CTE values in [13], we used $C^{Th}{}_{AA} = C^{Th}{}_{BB} = 14 \times 10^{-6}$ /K, and $C^{Th}{}_{AB} = 250 \times 10^{-6}$ /K for simulations with crystalline anisotropy (Figs. 4(b-d)). For isotropic simulations (Fig. 4(a)), we used $C^{Th}{}_{AA} = C^{Th}{}_{BB} = C^{Th}{}_{AB} = 93 \times 10^{-6}$ /K corresponding to the same net volume expansion as in the anisotropic case.

20. Bead-size N is representative of the number of atoms each bead comprises of. Equating bond-length b^0 to the edge of a cubic bead of size N implies its $N^{1/3}$ scaling. In our scheme the temperature k_BT and the ratio λ = *(bead oscillation amplitude)*/b^0 are independent of bead-size N. Therefore $K_{bond}(\lambda b^0)^2 \sim k_BT$ implies that K_{bond} scales as $N^{2/3}$. The fastest oscillation time $\tau_{fastest} \sim \sqrt{M/K_{bond}}$, which implies a scaling of $N^{5/6}$ (given that the bead mass M scales linearly with N).

21. See webpage: http://www.cs.sandia.gov/~sjplimp/lammps.html.

22. A. Donev, F. H. Stillinger, and S. Torqauto, *Phys. Rev. Lett.* **95**, 090604 (2005), and references therein.

23. L. Vanel et al., in *Physics of Dry Granular Media*, H. J. Herrmann, J. P. Hovi, and S. Luding (eds.), Kluwer Academic Publishers, Dordrecht, 1998.

24. P-G. de Gennes, *CR Acad. Sci.* (Paris) **327**, 267 (1999).

25. L. W. Vick and R. G. Kander, *Pol. Eng. Sci.* **38,** 1985 (1998).

26. Our approach is formally more similar to an atomistic force field than particle-based approaches that have been previously used to study continuum flow problems, e.g., smoothed particle hydrodynamics (SPH) [27], or its derivative, smooth particle applied mechanics (SPAM) [28].

27. J. Monaghan, *Ann. Rev. Astronomy and Astrophysics* **30**, 543 (1992).

28. W. G. Hoover and H. A. Posch, *Phys. Rev. E* **59**, 1770 (1999).

Table 1. Mesoscale parameters used in our simulations. Basic length and energy units are in μm and *kcal/mol* respectively. The mass unit is that of a mesoscale TATB bead ~ 1.94×10^{-12} gm, which implies $N \sim 10^{12}$ (in terms of # equivalent H-atoms per mesoscale bead).

Variable	Scaling	Physical Unit	Value
Fastest Oscillation Time ($\tau_{fastest}$)	$N^{5/6}$	1-10 *ms*	0.6
MD Time-step used	$N^{5/6}$	0.01-0.1 *ms*	0.006
Room temperature (k_BT)	N^0	*kcal/mol*	0.6
K_{bond}	$N^{2/3}$	$kcal/mol/(\mu m^2)$	100.0
K_{angle}	N^0	$kcal/mol/(rad^2)$	100.0
Eq. bond-length (b^0)	$N^{1/3}$	μm	1.0
Eq. angle (A^0)	N^0	*rad*	$\pi/2$
Morse-parameter D	N^0	*kcal/mol*	7-10
Morse-parameter α	$N^{1/3}$	μm^{-1}	10-60
Morse parameter r_0	$N^{1/3}$	μm	1.3

Figure captions:

Fig 1. Irreversible growth of polymer-bound TATB powder upon repeated thermal cycling between -54 °C and 74 °C for five different cylindrical samples cut (at different angles) out from the same TATB billet (shown as fractional change in linear dimension). (a) Plot for one of the samples showing length variation within each thermal cycle; (b) room-temperature length for all five samples within each thermal cycle.

Fig 2. (a) Experimental crystal structure of TATB. There are two molecules in each unit cell. Spatially extended models reveal a layered structure, with layers parallel to the plane of the aromatic rings. Color scheme: C (gray), N (blue), O(red), H(white); (b) equilibrium growth morphology of TATB obtained by minimizing the net surface energy; (c) an equivalent crystal of "meso" beads, with alternating planes of A and B-beads parallel to the XY planes of Fig. 1(a); (d) a typical TATB crystallite composed of meso beads used in our simulations.

Fig 3. Sample models of TATB powder with packed crystallites: (a) only large crystallites; (b) *pressed-powder:* large crystallites along with small cubic TATB particles.

Fig 4. Simulated irreversible growth of TATB pressed-powder using our mesoscale model [structure of Fig. 3(b)]. (a) Plot showing the length variation with repeated thermal cycling over the experimental temperature range of -54 ^{o}C and 74 ^{o}C *in the absence of crystalline anisotropy.* The parameter values: D = 7 and $\alpha = 40$. The room temperature values are indicated as solid circles. (b) Same as (a) *in the presence of crystalline anisotropy*. (c, d) Show the room temperature results [extracted from the thermal cycles similar to as shown by solid circles in (b)] for different values of D and α in the presence of anisotropy. (a, b) Display actual length dimensions of the simulation ensemble, while (c, d) represent fractional change in linear dimensions (similar to that shown in Fig 1). Units of D and α are in kcal/mol and μm^{-1} respectively.

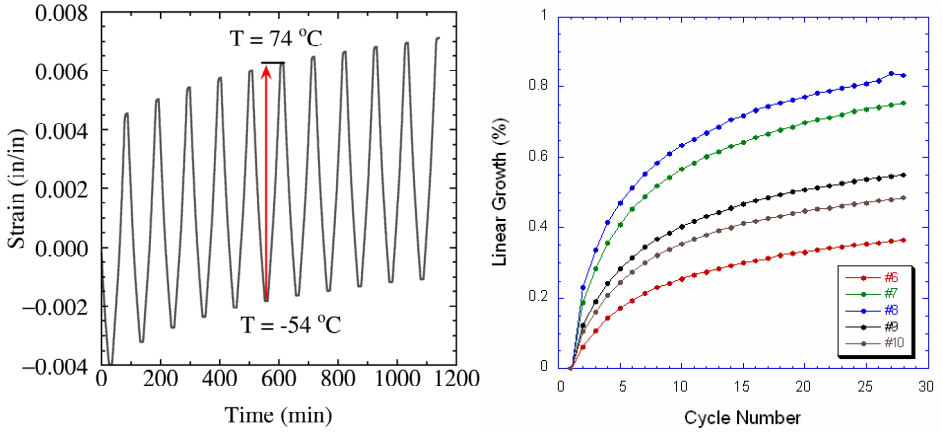
0.008
0.006
0.004
0.002
0.000
−0.002
−0.004
Strain (in/in)
T = 74 °C
T = -54 °C
0
200
400
600
800
1000
1200
Time (min)
1
0.8
0.6
0.4
0.2
0
Linear Growth (%)
#6
#7
#8
#9
#10
0
5
10
15
20
25
30
Cycle Number

(a) (b)

Figure 1

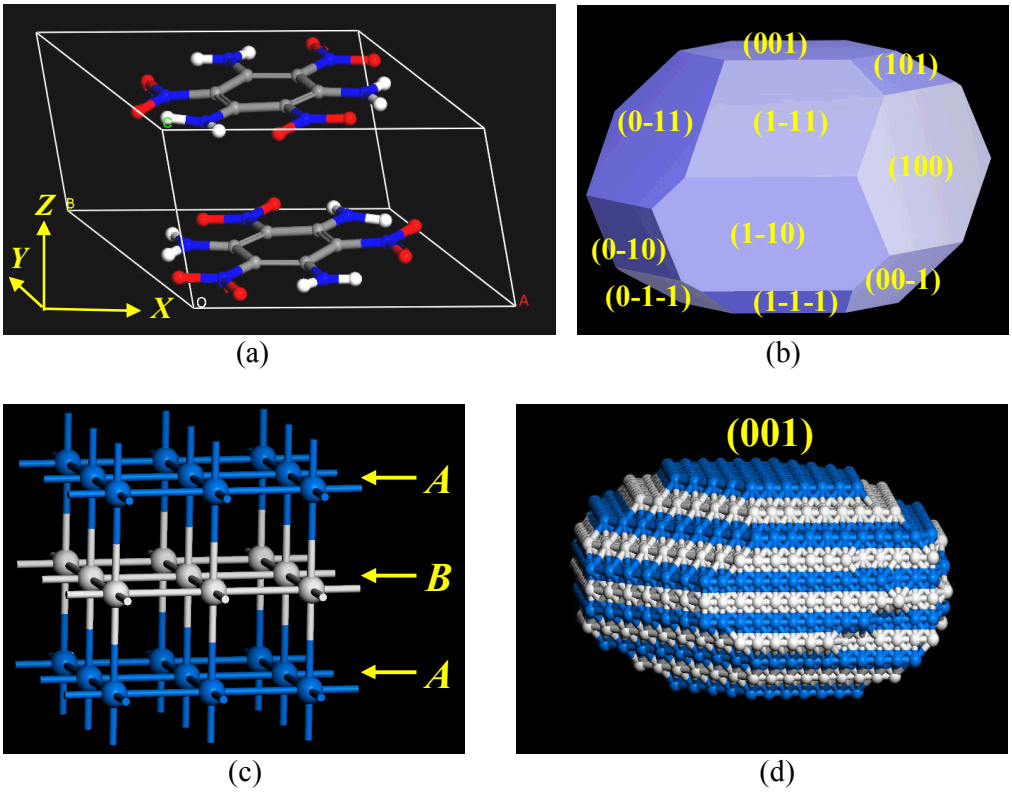

(a) (b)

(c) (d)

Figure 2

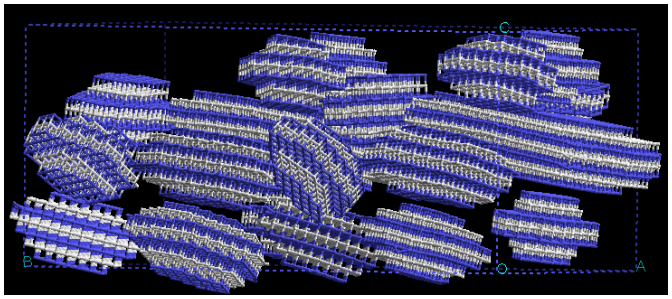

(a)

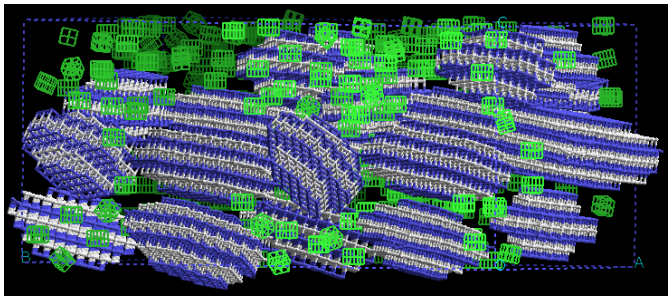

(b)

Figure 3

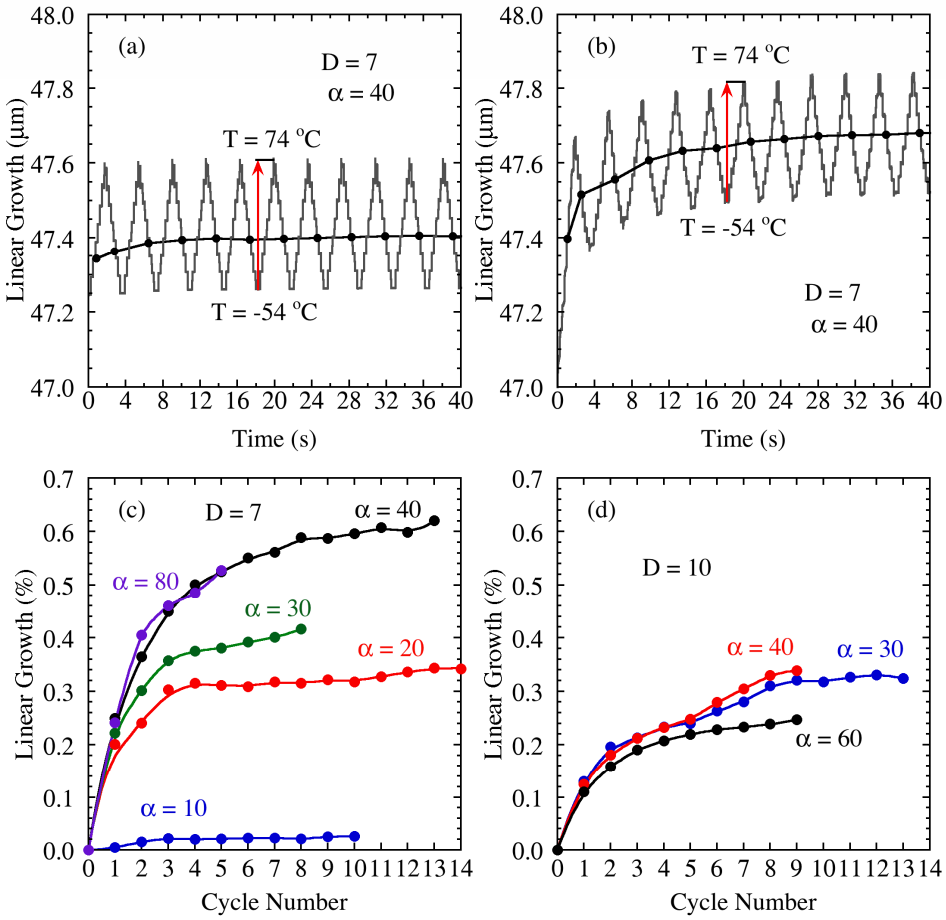
(a)
D = 7
α = 40
T = 74 °C
T = -54 °C
Linear Growth (μm)
Time (s)
(b)
T = 74 °C
T = -54 °C
D = 7
α = 40
Linear Growth (μm)
Time (s)
(c)
D = 7
α = 40
α = 80
α = 30
α = 20
α = 10
Linear Growth (%)
Cycle Number
(d)
D = 10
α = 40
α = 30
α = 60
Linear Growth (%)
Cycle Number

Figure 4